Plasma Physics and
Controlled Fusion

PURPOSE-LED
PUBLISHING™

PAPER • **OPEN ACCESS**

Comparison of deconvolution techniques for 1D neutron emission profile reconstruction using ITER Radial Neutron Camera synthetic data and JET neutron camera measurements

To cite this article: Katarzyna Mikszuta-Michalik *et al* 2025 *Plasma Phys. Control. Fusion* **67** 045017

View the article online for updates and enhancements.

You may also like

- Conceptual design of a camera system for neutron imaging in low fusion power tokamaks
X. Xie, X. Yuan, X. Zhang et al.
- Combined unfolding and spatial inversion of neutron camera measurements for ion temperature profile determination in ITER
D. Marocco, B. Esposito and F. Moro
- Conceptual design of the high resolution neutron spectrometer for ITER
Marek Scholz, Anders Hjalmarsson, Leszek Hajduk et al.

This content was downloaded from IP address 81.57.8.77 on 01/10/2026 at 14:47

OPEN ACCESS
IOP Publishing
Plasma Physics and Controlled Fusion
Plasma Phys. Control. Fusion **67** (2025) 045017 (13pp)
https://doi.org/10.1088/1361-6587/adbd73

Comparison of deconvolution techniques for 1D neutron emission profile reconstruction using ITER Radial Neutron Camera synthetic data and JET neutron camera measurements

Katarzyna Mikszuta-Michalik[1,*], Daniele Marocco[2], Basilio Esposito[2] and JET Contributors[3]

[1] Institute of Plasma Physics and Laser Microfusion, Hery Street 23, 01-497 Warsaw, Poland
[2] ENEA, Nuclear Department, C. R. Frascati, Via E. Fermi 45, I-00044 Frascati, Roma, Italy

E-mail: katarzyna.mikszuta@ifpilm.pl

Received 23 October 2024, revised 24 February 2025
Accepted for publication 6 March 2025
Published 14 March 2025

Abstract

The primary purpose of the ITER Radial Neutron Camera (RNC) is the real-time control of plasma burn. It requires neutron emissivity profile reconstruction with an accuracy better than 10% and a time resolution of 10 ms. Algorithms based on the Tikhonov Regularization, Minimum Fisher Information, Maximum Entropy and Maximum Likelihood methods were compared for the 1D deconvolution of the neutron emissivity profile from RNC measurements. The reconstruction performance was evaluated using the baseline RNC architecture and two ITER DT 15 MA scenarios of inductive operation. The reconstruction was carried out assuming constant neutron emissivity on the magnetic flux surfaces: in this case, the neutron profile can be represented as a normalized poloidal magnetic flux function. The number of the used flux surfaces was about twice the number of lines of sight in the RNC. All methods (except Maximum Entropy) achieved a reconstruction accuracy better than 10%. The two Tikhonov Regularization algorithms provide in general a good reconstruction, with the second-order derivative regularization matrix giving a better accuracy than 10% in a wider range of the normalized poloidal magnetic flux (Ψ) but a higher standard deviation than the first-order derivative regularization matrix. At the same time, the Minimum Fisher Information proved to be the most stable method. The performance of these two best methods was validated with actual experimental data using the JET neutron camera measurements collected in the second deuterium-tritium campaign.

[3] See Maggi et al 2024 (https://doi.org/10.1088/1741-4326/ad3e16) for JET Contributors.
[*] Author to whom any correspondence should be addressed.

Original content from this work may be used under the terms of the Creative Commons Attribution 4.0 licence. Any further distribution of this work must maintain attribution to the author(s) and the title of the work, journal citation and DOI.

© 2025 The Author(s). Published by IOP Publishing Ltd

Keywords: Radial Neutron Camera, ITER, JET, neutron diagnostics, neutron emissivity, deconvolution

1. Introduction

The ITER Radial Neutron Camera (RNC) is a fan-shaped set of collimators equipped with neutron detectors providing line-integrated neutron measurements. The primary purpose of the RNC is the real-time reconstruction of the neutron emissivity profile with 10 ms time resolution and 10% accuracy for plasma burn control purposes. The neutron emissivity data associated to each 10 ms time bin shall be delivered to the plasma control system with a maximum delay (latency) of 5 ms. The diagnostic is also expected to provide measurements of the fusion power density, ion temperature profile and fuel ratio profile (n_D/n_T) [1]. The baseline ITER RNC architecture consists of 22 detectors (see figure 1) [2].

The RNC will measure the two-dimensional spatial distribution of neutron emissivity in a whole tokamak poloidal cross-section. If the ion velocity can be assumed as characterized by a Maxwellian distribution, then ion temperature, ion density and neutron emissivity profiles are constant on the flux surfaces, and the two-dimensional problem of the neutron emissivity reconstruction can be reduced to one dimension. This assumption may not be valid if the neutron emissivity is not symmetric, for example, in the case of plasma instabilities or non-thermal plasmas.

The RNC performance has already been evaluated through 1D and 2D neutron emissivity reconstruction techniques [2]. 2D tomography using Minimum Fisher Regularization [3] is time-consuming and more suited for off-line analysis. For real-time analysis, 1D reconstruction is used, and real-time application of the MSST [4] code based on the Tikhonov Regularization with the first derivative operator has been implemented, using 20 flux surfaces (a quantity smaller than the number of the detectors) [5].

The present work aims to characterize the quality of different reconstruction techniques in terms of accuracy, robustness and computation time and to guide the selection of the most suitable method for the real-time application. Four 1D neutron emissivity reconstruction techniques are analyzed, namely: Tikhonov Regularization, Minimum Fisher Information, Maximum Entropy and Maximum Likelihood. The algorithms employed for this analysis were originally developed for neutron spectrum reconstruction from activation measurement [6].

For their validation, the reconstruction methods were applied to actual experimental data collected by the JET neutron camera. The JET neutron camera consists of two fan-shaped collimating structures observing plasma vertically and horizontally (see figure 2). It allows the reconstruction of asymmetrical neutron emissivity profiles. Each collimator is equipped with a NE213 liquid organic scintillator with pulse Shape Discrimination (PSD) electronics for simultaneous recording of the 2.5 MeV and 14.1 MeV neutron emission and a BC418 plastic scintillator for the measurement of 14.1 MeV neutrons [7]. The neutron emissivity reconstruction methods were applied to the analysis of sawtooth crashes in JET baseline scenario experiments in the second JET deuterium–tritium campaign (DTE2) [8, 9].

The paper is organized as follows: section 2 describes the reconstruction methods, section 3 discusses the RNC synthetic measurement, section 4 provides the reconstruction results for synthetic data, section 5 shows the reconstruction results obtained for the JET neutron camera experimental data, and section 6 summarizes the outcomes of the analysis.

2. Reconstruction methods

The reconstruction of the neutron emissivity profile is an ill-posed and ill-conditioned inverse problem that can be described by the following equation:

$$\sum_i G_{ij} f_i = d_j \tag{1}$$

where $\boldsymbol{G}$ is the contribution matrix that describes the geometry of fields of view and contribution from each flux surface to the measurement, includes volumes of truncated cones seen by the detectors with solid angles taken into account [m^3] (matrices used in the presented analysis include only geometrical effects, but it can be calculated by MCNP simulation), f_i is the neutron emissivity value associated with the ith magnetic surface [$n \cdot s^{-1} \cdot m^{-3}$], and the d_j is the neutron rate measured by the jth detector [$n\ s^{-1}$].

The problem of the reconstruction f from d has no unique solution. Therefore, the inversion is very sensitive to measurement errors, including counting statistics and background connected with the scattered neutrons. The codes written in Python programming language developed in [6] were used for the 1D neutron emissivity reconstruction. The matrix elements G_{ij} are defined as the intersection volumes of fields of view with flux surfaces with solid angles taken into account. The analysis was carried out for a number of magnetic flux surfaces equal to 40, which is almost two times higher than in the MSST code analysis [5]. Using a higher number of flux surfaces increases the spatial resolution of the reconstruction, by enabling the capability to resolve smaller structures and the reconstruction accuracy. On the other hand it makes the calculation more challenging since it increases the degree of ill-posedness and the computation time.

The first algorithm proposed for the analysis is based on the Tikhonov Regularization (TR) method, also known as ridge regression. It is the least square method extended by a side constraint:

$$\vec{f} = \min\left(||\boldsymbol{G}\vec{f} - \vec{d}||_2 + \lambda^2 ||\boldsymbol{L}\vec{f}||_2 \right) \tag{2}$$

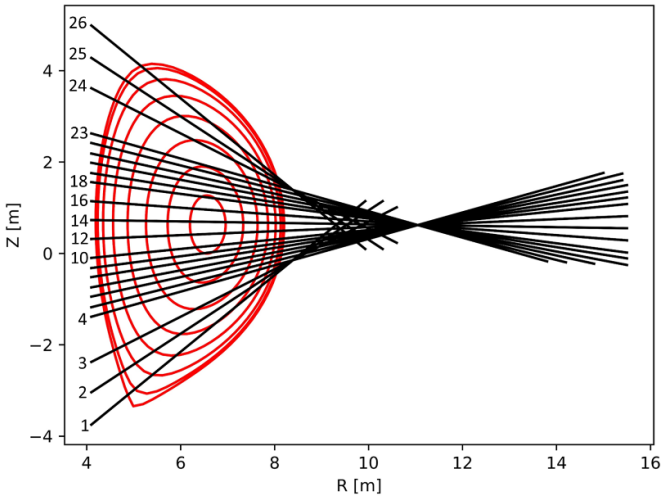


Figure 1. The layout of the lines of sight (LOS) of the ITER RNC baseline architecture presented with magnetic field contours for ITER DT 15 MA scenario. Note that LOS # 11, 13, 15 17 are not represented since they are dedicated to two other diagnostics interfacing with the RNC:—Radial Gamma Ray Spectrometer (RGRS) and High Resolution Neutron Spectrometer (HRNS).

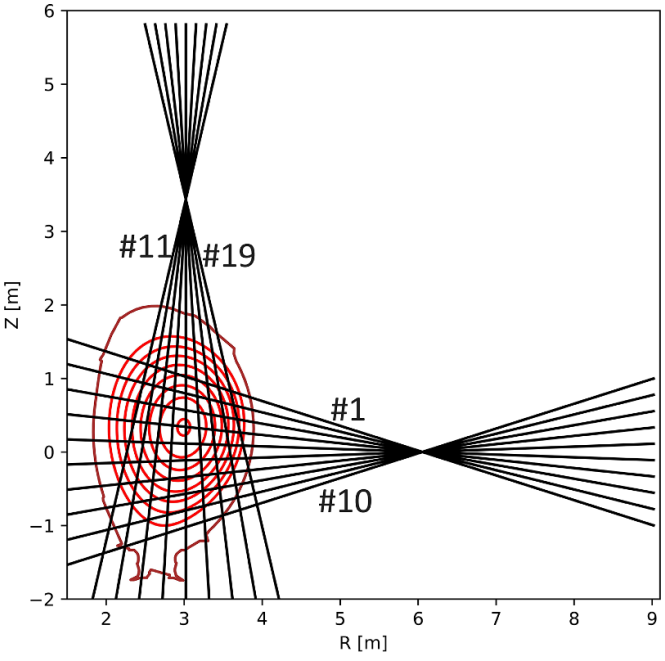


Figure 2. The layout of the LOS of the JET neutron camera presented with magnetic field contours and first wall for discharge #99523 (time slice $t = 50.49$ s).

where λ is the regularization parameter, and $\boldsymbol{L}$ is the regularization matrix in the form of a first or second-order derivative operator.

The first-order derivative operator minimizes the gradient between adjacent points of the profile. The second-order derivative operator corresponds to the Laplacian filter [10]. The minimization of equation (2) is performed by lower-upper (LU) decomposition. The regularization parameter λ is optimized by the L-curve method [11].

The other three algorithms are based on the Minimum Fisher Information (MFI), Maximum Entropy (MaxEnt), and Maximum Likelihood (ML) methods. They are iterative and require a default profile (initial guess) as input.

MFI is a special version of the TR algorithm with a regularization matrix defined as Fisher Information that is an estimator of the degree of the expected error in the measurement, defined as the combination of the derivative matrix ($\boldsymbol{L}$) with the weight matrix ($\boldsymbol{W}$):

$$\boldsymbol{I_F} = \boldsymbol{L^T W L}. \tag{3}$$

The weight matrix at iteration $k + 1$ is inversely proportional to the solution from iteration k (f_i^k):

$$W_{ij} = \frac{1}{f_i^k}\delta_{ij} \qquad \text{for } f_i^k > 0 \tag{4}$$

where δ_{ij} is Kronecker delta.

Therefore, the elements of the regularization matrix that correspond to small absolute values of the solution (at least an order of magnitude lower than maximal emission) are associated with a large smoothing. Such method reduces the probability of filtering out peaked structures and decreases the influence of the edges on the rest of the profile [12]. The calculation of the regularized solution and optimization of the regularization parameter is performed similarly as in TR. The stopping criterion is Pearson χ^2 equal to 1 with two decimal places precision.

The MaxEnt method is based on the entropy definition from information theory. The entropy of the count rates measures the uncertainty of the neutron emissivity reconstruction. The disadvantage of the MaxEnt method is the lack of a physical basis. The advantage is the requirement of the solution's positivity-defined values to be automatically applied to MaxEnt because the entropy does not exist for negative parameters. MaxEnt is also a regularization algorithm similar to TR with matrix $\boldsymbol{L}$ in the form of entropy. The regularization operator is a diagonal matrix with elements defined as:

$$L_{ii} = f_i - f_i^0 - \ln f_i/f_i^0 \tag{5}$$

where f_i^0 is the default profile.

Calculations are based on the SVD (Singular Value Decomposition), which automatically reduces the impact of input data with higher uncertainties. The χ^2 and the trace of the entropy matrix are calculated for a wide range of λ parameter values. From the set of the results with χ^2 closest to one, one with maximal entropy is selected as optimal [13].

The last developed algorithm is based on Maximum Likelihood (ML) method. A likelihood function describes the reliability of the uncertainty of the neutron emission profile. The function can be defined as hypothesis that f give measurement data d—$P(d|f)$. The ML method leads to a determination of the neutron emission profile with the highest probability. The ML algorithm is based on the equation introduced by Shepp and Vardi [14] for the probability distribution that the

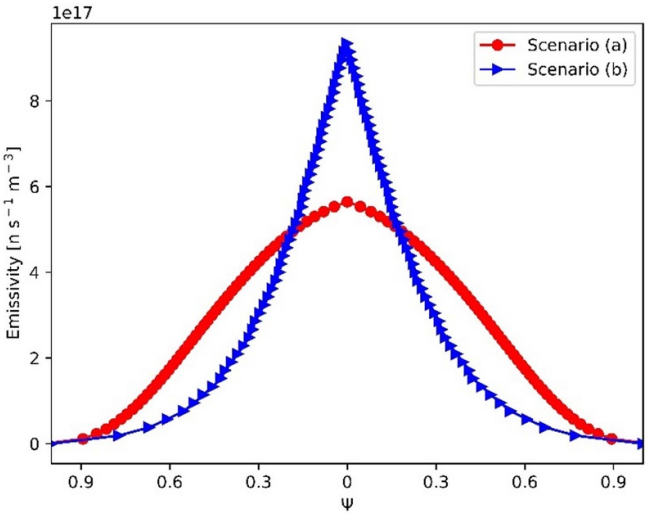


Figure 3. Neutron emissivity profiles for two ITER DT 15 MA scenarios of inductive operation (red circles—scenario (a), blue triangles—scenario (b)).

Poisson statistic can describe:

$$f_i^{k+1} = \frac{f_i^k}{\sum_j G_{ji}} \sum_j \frac{d_j}{\sum_n G_{jn} f_n^k} G_{ji} \tag{6}$$

where k denotes the number of iterations, and n is the summation index over detectors.

3. Synthetic measurement

The simulation of RNC measurements was made for two ITER DT 15 MA scenarios of inductive operation; scenario (a) with 4.5 keV pedestal temperature and scenario (b) with peaked density (see figure 3) [4]. The synthetic data (presented in figure 4 and [3]) were produced according to the procedure described in [15] based on neutron emissivity inputs provided by ITER Organization [16]. Before the reconstruction analysis, Poisson random noise and a background term due to scattered neutrons (evaluated by means of MCNP calculations) are added to the synthetic data. The magnitude of the Poisson noise is associated with the counts recorded by each LOS in 10 ms (time resolution requirement for real-time reconstruction of the neutron emissivity profile).

4. Reconstruction results for synthetic data

The four algorithms described in section 2 were applied to reconstruct the neutron emission profiles from ITER RNC synthetic measurement. The final result of the calculation is the average value over 100 reconstructions; each reconstruction is performed with data differing by systematic and random noise. The input data to the reconstruction was prepared starting from the count rates reported in figure 4 and adding to them the systematic noise term due to background from collided neutrons evaluated through MCNP and the random noise term due to Poisson statistics (10 ms time resolution). The performance of the different reconstruction algorithms was evaluated using the following parameters:

- Reconstruction accuracy, defined for each magnetic flux surface as:

$$A_i = \left| \frac{f_{\text{mean}\,i} - S_i}{S_i} \right| \tag{7}$$

  where S_i is the neutron emissivity simulated for ith magnetic flux surface, and $f_{\text{mean}\,i}$ is final result for ith magnetic flux surface,
- Standard deviation of accuracy that is represented by error bars on figures,
- RMS (root mean square) is used as a figure of merit in comparison of the reconstruction performance:

$$\text{RMS} = \sqrt{\frac{1}{n}\left(A_1^2 + A_2^2 + \ldots + A_n^2\right)} \tag{8}$$

  where n is the number of the magnetic flux surfaces considered in the reconstruction (40 in this analysis).
- Distance from 10% limit—the average difference between the upper edge of the error bar and the 10% limit.
- Time of the computation performed on PC with of Intel(R) Core(TM) i5-8350 U and 16GB RAM. The CPU time of the algorithm was automatically measured by Python. The time measurement was considered only for comparison between algorithms.

The dotted horizontal grey lines in figures 5, 6, 8, 10, and 11 indicate the 10% accuracy level, which is the requirement for the real-time burn control.

The reconstruction results obtained by the TR method for scenarios (a) and (b) with the application of the first or second-order derivative are presented in figures 5 and 6, respectively. The standard deviation for the second-order derivative is higher, but accuracy is better than 10% in a wider range of the normalized poloidal magnetic flux (Ψ). The application of the first-order derivative matrix as the side constraint provides the final result with accuracy better than 10% on the core (up to $\Psi \sim 0.65$), but the edge is less accurately reconstructed. In general, the accuracy of the final result obtained by the TR method with the second-order derivative is better than 10% up to normalized poloidal magnetic flux (Ψ) around 0.9. The standard deviation of the calculation is higher for scenario (b), which is steeper and, therefore, more challenging to reconstruct. The CPU time of calculation is about 0.07 s.

The default profiles used for emissivity profile reconstruction with the three iterative algorithms are presented in figure 7. For the reconstruction of profile (a) the (b) profile, and a flat profile were used. Analogously, in the case of profile (b), the default profiles were the (a) profile and the flat profile. The flat profile was included to verify the reconstruction capability of the algorithms when starting from a profile very different from the original one.

The results of the reconstruction performed by the MFI method are presented in figure 8 for scenarios (a) and (b). The discrepancies between the results obtained with different

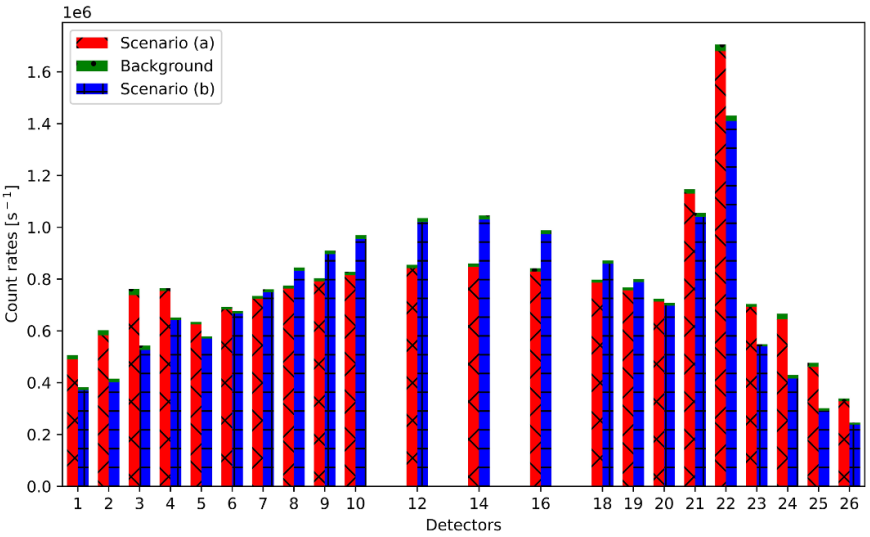


Figure 4. Simulated count rates and background for ITER RNC [3]. Note that the count rate is high in some channel (e.g. 21 and 22) for geometric reasons: such channels have shorter collimators.

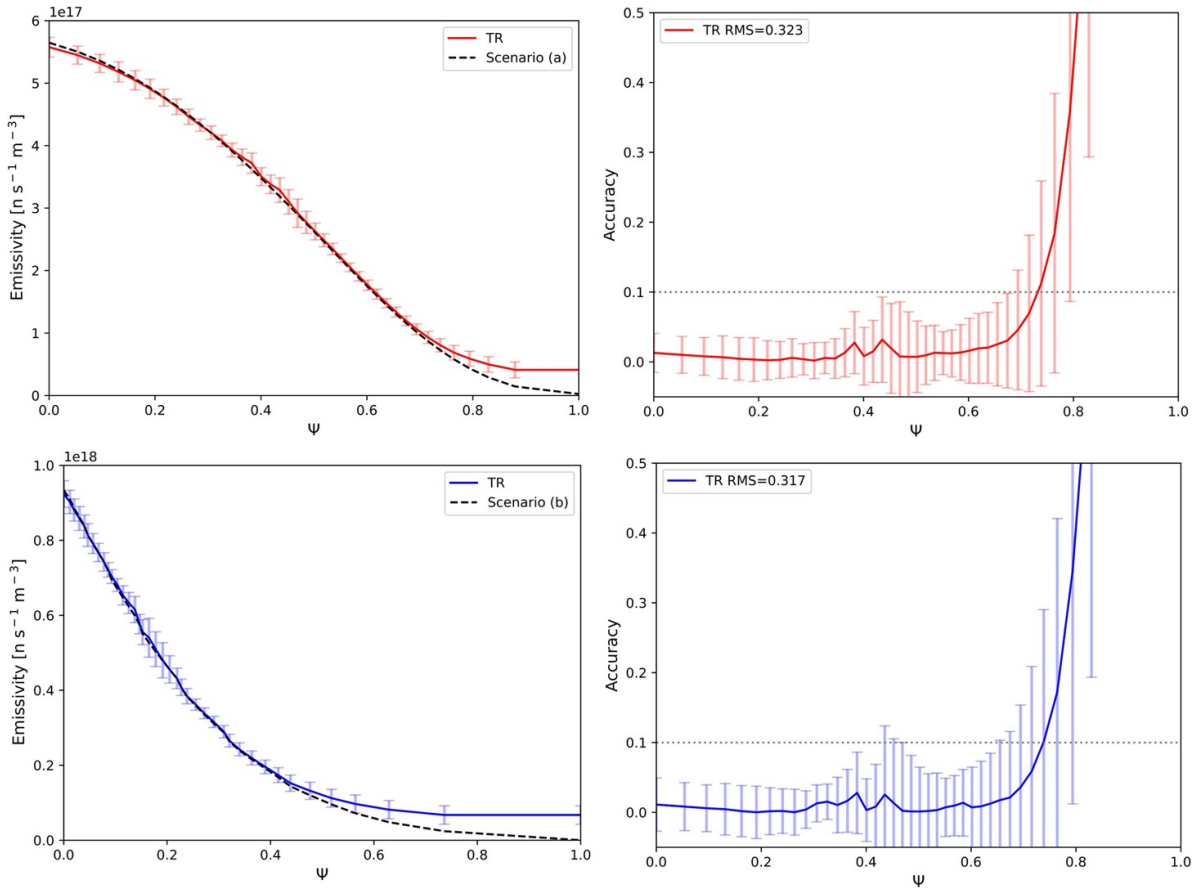


Figure 5. Neutron emissivity profile reconstruction obtained by the TR method with the first-order derivative regularization matrix for scenario (a) (top) and scenario (b) (bottom): comparison between the original emissivity profile and the average reconstructed profile with 1 standard deviation error (left); profile of the reconstruction accuracy with 1 standard deviation error (right).

default profiles can be observed only at the plasma edge for scenario (a). The reconstructed neutron emission distributions are the same in the case of scenario (b). The RMSs obtained by the MFI are higher than in the TR analysis, but the standard deviation is smaller. The accuracy is better than 10% up to 0.8 Ψ. The CPU time on used PC is about 80 ms.

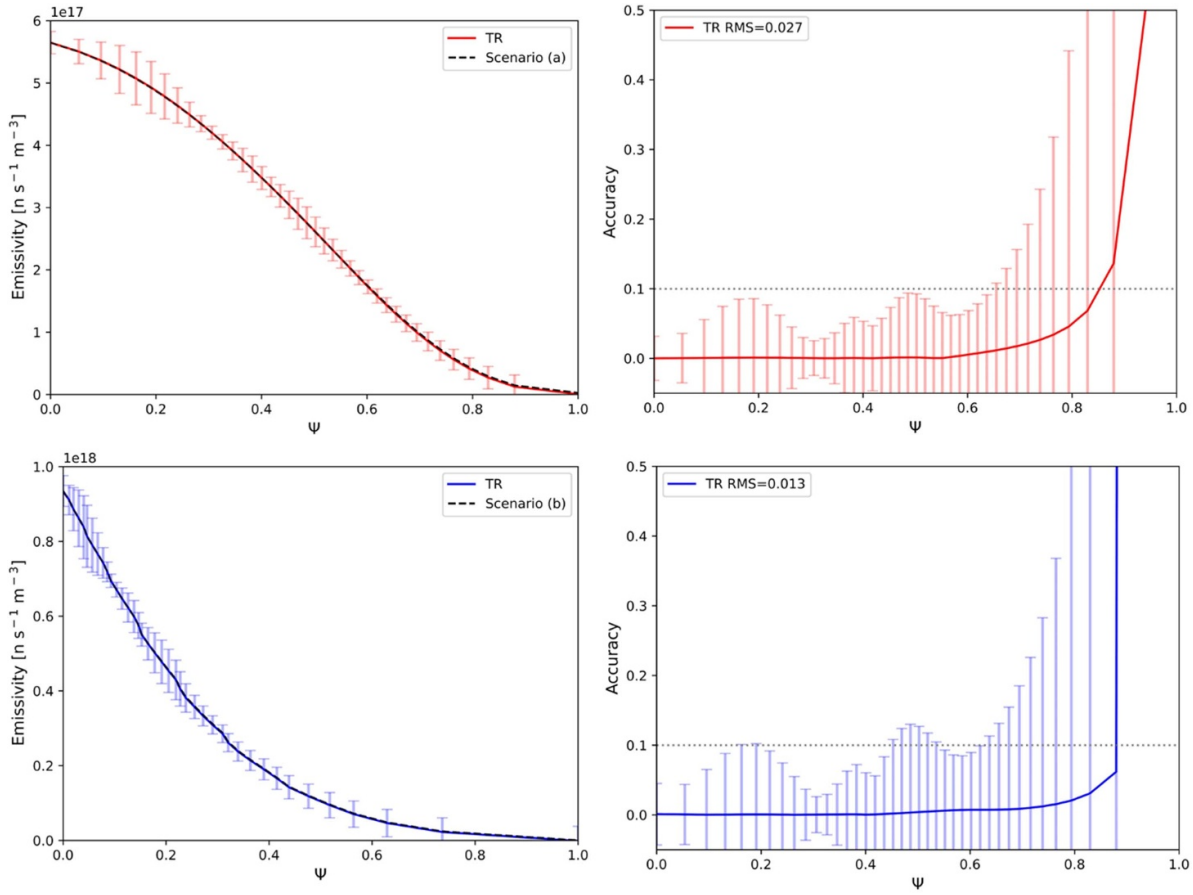


Figure 6. Neutron emissivity profile reconstruction obtained by the TR method with the second-order derivative regularization matrix for scenario (a) (top) and scenario (b) (bottom): comparison between the original emissivity profile and the average reconstructed profile with 1 standard deviation error (left); profile of the reconstruction accuracy with 1 standard deviation error (right).

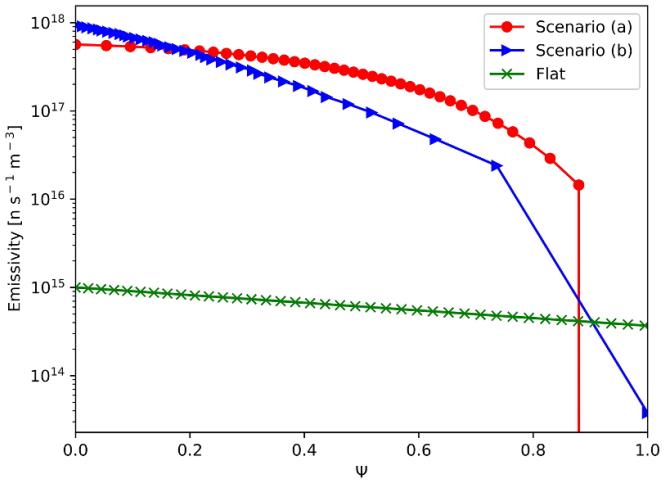


Figure 7. Default profiles used for neutron emissivity reconstructions with MFI, MaxEnt, and ML algorithms.

No reasonable reconstruction results were obtained with the MaxEnt algorithm. The solution obtained with the regularization parameter identified with the discrepancy principle in the default range used for the analysis (10^{-1}–10^{-9}) is oversmoothed and flat, indicating that the regularization imposed by the entropy matrix is too strong (see example on figure 9). If, in the attempt to obtain a sensible solution, the range of the regularization parameter is reduced and limited to extremely small values ($<10^{-9}$), the solution immediately falls into an excessively noisy profile, which essentially coincides with the least square solution of the linear system, as shown in figure 10. No stable and sensible solution was found by scanning different possible values of the regularization parameter range. In this case, the regularization matrix based on the entropy definition does not provide reliable reconstruction.

The results obtained by the ML method are presented in figure 11 for scenarios (a) and (b). The ML algorithm is very sensitive to the default profile. The accuracy of the result obtained for scenario (a) using scenario (b) as default profile is better than 10% in the whole plasma poloidal cross-section. In the case of scenario (b), the profile reconstructed with scenario (a) as default profile has accuracy better than 10% up to 0.9 normalized poloidal magnetic flux. The usage of the flat default profile gave the required accuracy only up to 0.4 Ψ. The computation time strongly depends on the required number of iterations for one dataset but does not exceed 1 s CPU time. The mean standard deviations are very small (<0.1).

Table 1 compares, for the different algorithms, the obtained RMS, the maximal normalized poloidal flux with an accuracy below 10%, distance from 10% limit and the CPU

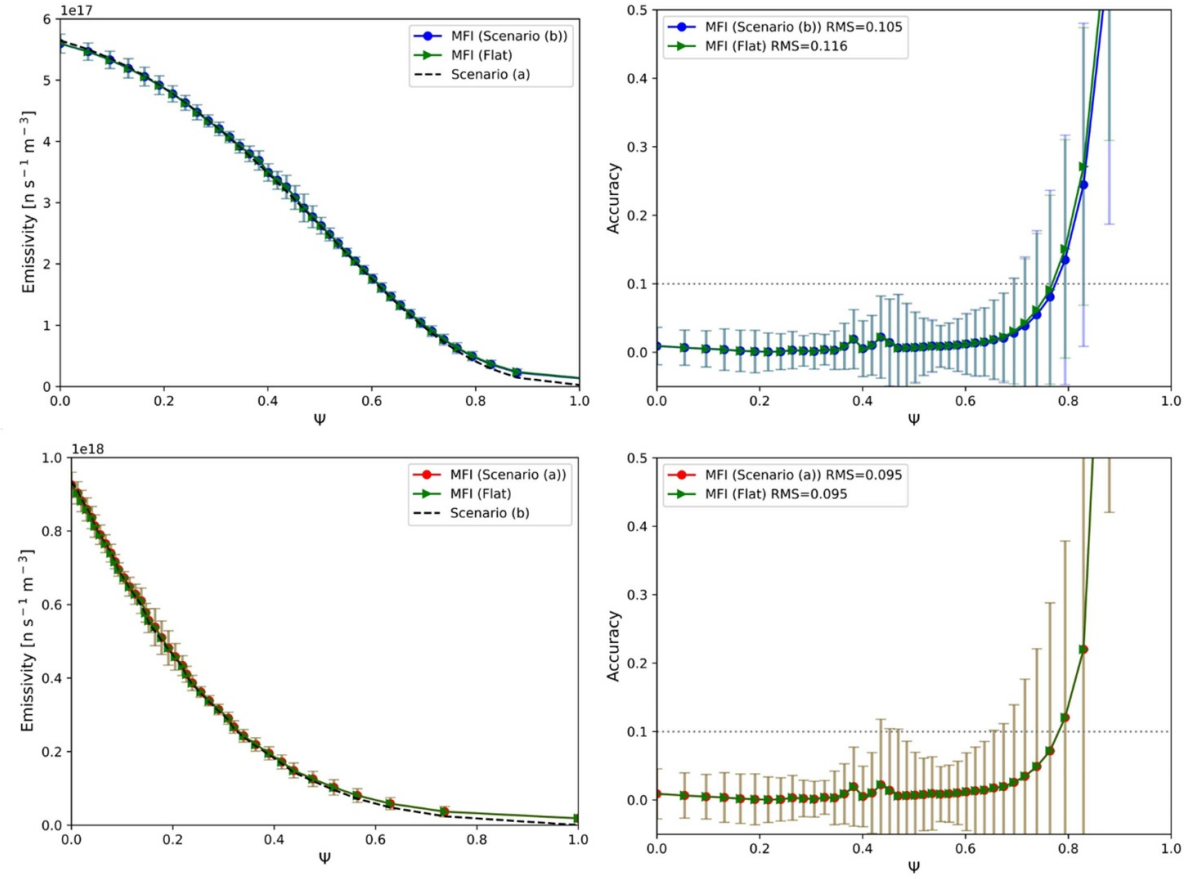


Figure 8. Neutron emissivity profile reconstruction obtained by the MFI method for scenario (a) (top) and scenario (b) (bottom): comparison between the original emissivity profile and the average reconstructed profile with 1 standard deviation error (left); profile of the reconstruction accuracy with 1 standard deviation error (right).

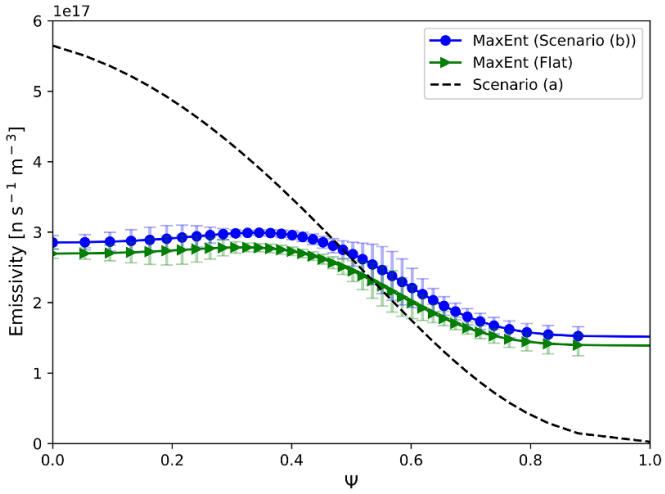


Figure 9. Emissivity profile reconstruction obtained by the MaxEnt method with automatic selection of the regularization parameter for scenario (a): comparison between the original emissivity profile and the average reconstructed profile with 1 standard deviation error.

time. Due to the excessive discrepancy between original and reconstructed profiles the MaxEnt algorithm was excluded from the comparison.

The lowest RMS was obtained by the TR method with the second-order derivative as a regularization matrix. The accuracy exceeds 10% only at the plasma edge, where the emissivity is very low compared to the core. The disadvantage of this method is the high standard deviation in case of steep profile reconstruction and negative distance from 10% limit. This observation indicates the low stability of the method.

MFI method is fast, weakly dependent on the default profile (effects are observed only on the plasma edges) and stable (the

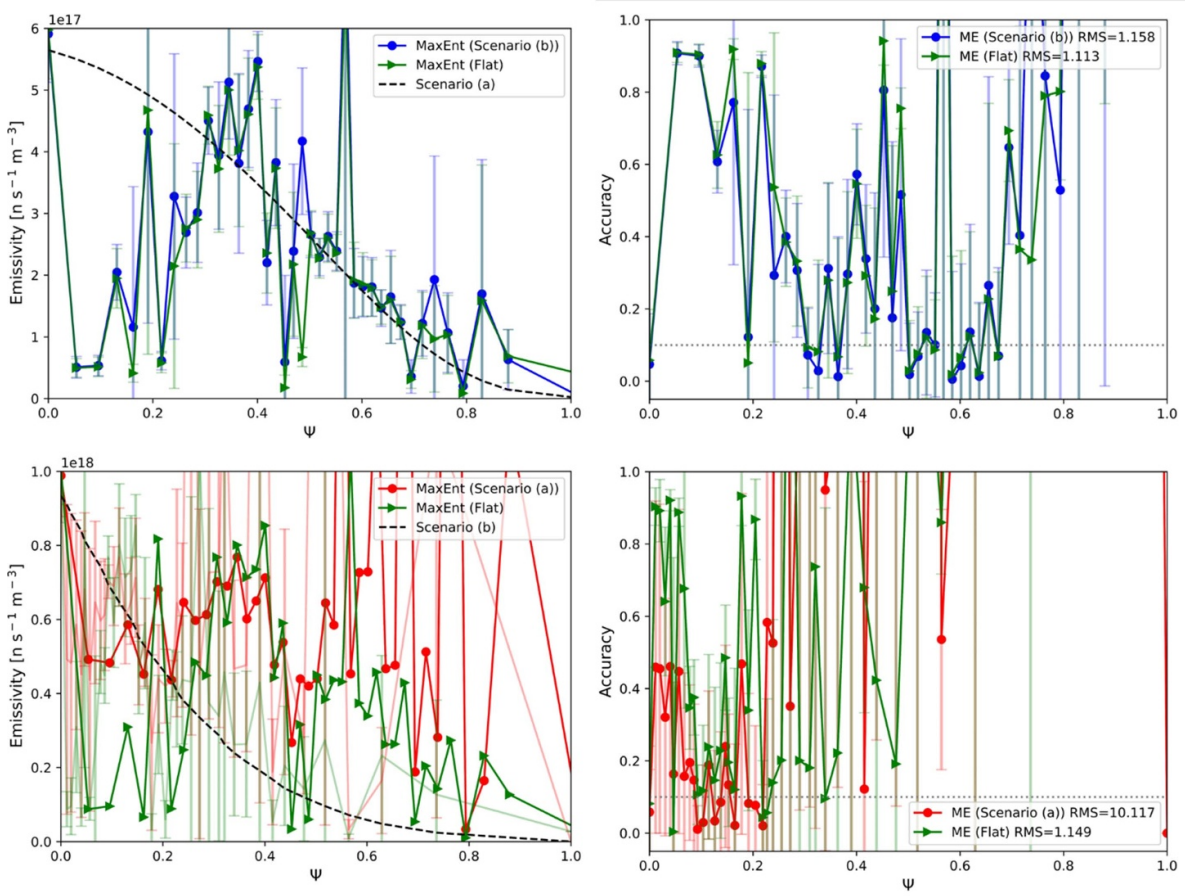


Figure 10. Emissivity profile reconstruction obtained by the MaxEnt method for scenario (a) (top) and scenario (b) (bottom): comparison between the original emissivity profile and the average reconstructed profile with 1 standard deviation error (left); profile of the reconstruction accuracy with 1 standard deviation error (right).

standard deviations of the mean profile from 100 reconstructions are similar for the different profile types). The distance from the 10% limit is low and equal to 0.03.

The ML method is susceptible to the default profile. If the default profile is similar to the original profile, the results meet the 10% accuracy requirement. There is a high risk of an unreliable solution if the default profile is very different from original one. The results require additional smoothing that might cause loss of the profile structures, e.g. sudden intensity peaks. The instability and the longest computation time make this method not suitable for online burn control on ITER.

The results indicate that TR and MFI algorithms are the best candidates for 1D real-time reconstruction of the neutron emissivity profile but also suggest to enable an option in the MSST regularization matrix to select both the first derivative and second derivative operator in order to have a reference for comparison.

5. Reconstruction results for the JET neutron camera

In this Section a validation of TR and MFI algorithms is carried out using actual experimental data from the JET neutron camera.

Sawtooth crashes were observed frequently during the JET baseline scenario experiments in DTE2. Such MHD activity is connected with the sudden ion temperature drop in the plasma core, which can be observed by neutron diagnostics as a neutron rate drop and neutron emissivity profile flattening or hollowing [17]. Sawtooth crashes are ideal to test the neutron emissivity reconstruction capability of the algorithms in the case of peaked (pre-sawtooth) and flattened emissivity (post-sawtooth).

The TR and MFI methods were applied to the analysis of the experimental data collected by the BC418 scintillators in the JET discharge #99523. The neutron rates for each detector were uploaded from the JET data base and pile-up correction was performed. The background correction was not included in the calculations due to the assumption that backscattering and in-scattering neutrons have negligible impact to the measurement in consequence of high energy threshold of BC418 scintillators. The outcomes of the reconstructions are provided as relative emissivity values due to the lack of actual geometrical calibration. The number of flux surfaces considered by the reconstruction algorithms was set to 25.

We consider the sawtooth crashes observed at three times: $t = 48.80$ s, $t = 49.73$ s and $t = 50.57$ s. The normalized neutron rate measured by the neutron monitors [18] and central

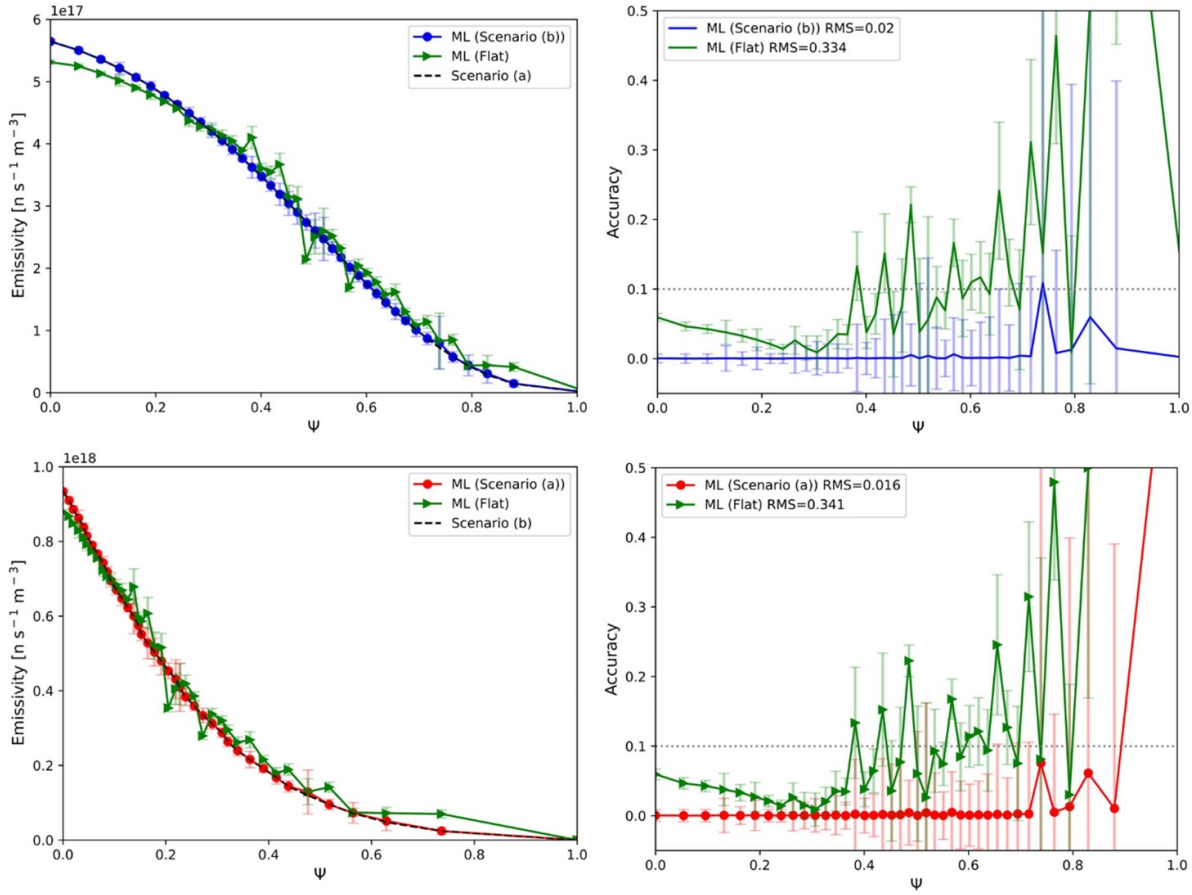


Figure 11. Emissivity profile reconstruction obtained by the ML method for scenario (a) (top) and scenario (b) (bottom): comparison between the original emissivity profile and the average reconstructed profile with 1 standard deviation error (left); profile of the reconstruction accuracy with 1 standard deviation error (right).

Table 1. Comparison of the RMS, maximal normalized poloidal flux with the accuracy below 10%, distance from 10% limit and CPU time obtained in the reconstruction by the different methods.

Method	Input data	Default profile	RMS	Maximal Ψ with 10% of accuracy	Distance from 10% limit	CPU time [s]
TR	Scenario (a)	1st order derivative	0.323	0.74	0.11	0.07
		2nd order derivative	0.027	0.88	−0.18	
	Scenario (b)	1st order derivative	0.317	0.74	0.10	
		2nd order derivative	0.013	0.88	0.07	
MFI	Scenario (a)	Scenario (b)	0.105	0.79	0.03	0.08
		Flat	0.116	0.79	0.03	
	Scenario (b)	Scenario (b)	0.095	0.79	0.03	
		Flat	0.095	0.79	0.03	
ML	Scenario (a)	Scenario (b)	0.020	1.00	−0.01	1
		Flat	0.334	0.38	0.13	
	Scenario (b)	Scenario (b)	0.016	0.88	0.02	
		Flat	0.341	0.38	0.14	

detectors of the neutron camera (horizontal channel #4, vertical channel #15) are presented in figure 12 together with the indication of time of the crash. The time resolution of the neutron camera data in this analysis is 10 ms (much slower than the sawtooth crash duration). The example of the input data before and after sawtooth crash in $t = 48.80$ s is presented in figure 13.

The results obtained by the TR method with the first-order derivative, TR method second-order derivative and MFI method are shown respectively in figures 14–16. All three

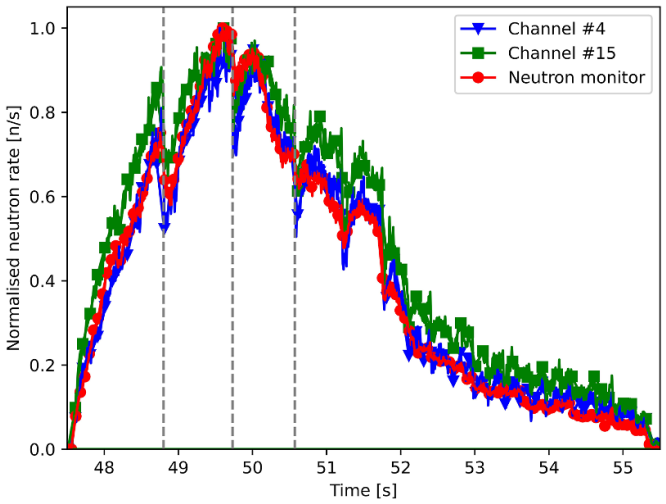


Figure 12. JET discharge #99523: normalized neutron rate measured by neutron monitor (red dots), channel #4 (blue triangles) and channel #15 (green squares) of neutron camera. Sawtooth crash times are indicated by the grey dashed lines.

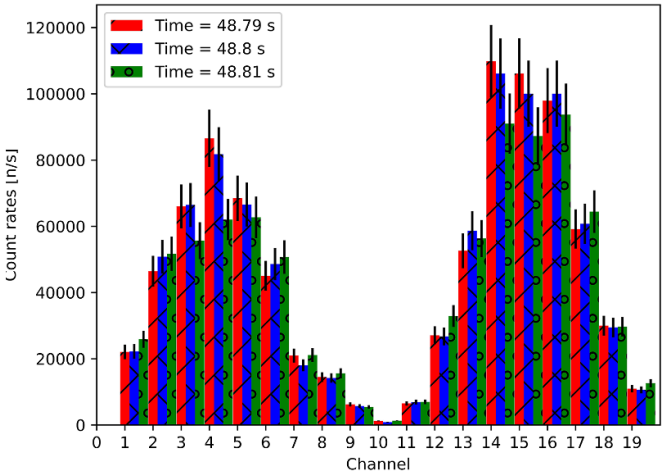


Figure 13. JET discharge #99523: neutron count rates measured by neutron camera before and after sawtooth crash in time = 48.80 s.

methods show the same trend of the changes in the neutron emissivity profile after the sawtooth crash, namely the flattening of the initially peaked profile. Due to the possible presence of asymmetries, the uncertainty of the reconstructed one-dimensional emissivity distribution is much higher than in the case of ITER synthetic data analysis. The source of the asymmetries are interactions with ions heated by auxiliary systems and MHD activity itself. The deviations from symmetry in ITER were not considered but can be investigated if a vertical camera is added to the analysis. This is the reason why, probably, we observe large differences in the peak value in the neutron emissivity depending on the reconstruction method (figure 17). The effect is lower in the case of the flattened profiles (figure 18). The average value of the discrepancy between the (peaked and flattened) emissivity reconstructed using the TR with the first-order derivative and MFI methods varies from 2% to 12%, whereas a difference exceeding 20% is found when comparing with the TR with the second-order derivative case. The TR method with the second-order derivative is characterized by a high standard deviation. That's why in JET less precise results are found compared to the TR method with the first-order derivative.

These JET experimental results therefore indicate that the Tikhonov Regularization with first-order derivative and Minimum Fisher Information methods provide a coherent reconstruction of neutron emissivities of different profile shapes and confirm the similar findings obtained with the RNC synthetic data emissivity reconstruction.

6. Conclusion

Four algorithms, initially developed for the reconstruction of neutron energy spectra from neutron activation measurements, have been applied for the 1D reconstruction of the neutron emission profiles in ITER tokamak using synthetic measurements calculated for the Radial Neutron Camera. The algorithms are based on the Tikhonov Regularization (with first and second-order derivative regularization matrix), Minimum Fisher Information, Maximum Likelihood and Maximum Entropy techniques.

The purpose of the analysis was the identification of more suitable methods for neutron emissivity profile reconstruction in real-time. The performance of the algorithms was evaluated in terms of reconstruction accuracy and CPU time. The two Tikhonov Regularization algorithms provide in general a good reconstruction, with the second-order derivative regularization matrix giving an accuracy better than 10% in a wider range of the normalized poloidal magnetic flux (Ψ) but a higher standard deviation than the first-order derivative regularization matrix. In addition, steeper profiles are more challenging to reconstruct using the Tikhonov Regularization with the second-order derivative regularization matrix. The Minimum Fisher Information method is less sensitive to the noise in the data and provides the best result for steep profiles. The Maximum Likelihood algorithm is the slowest and is very sensitive to the default profile, thus requiring a careful input selection. The Maximum Entropy algorithm was found to be unstable, and it was not possible to obtain any sensible reconstruction of the selected neutron emissivity profiles.

The Tikhonov Regularization and Minimum Fisher Information methods were selected for further investigation and validation against experimental data. The JET discharge #99523 from the second JET deuterium-tritium campaign was analyzed by means of these two methods.

The change from peaked to flattened neutron emission profile observed in sawtooth crashes of this discharge was used as a test of the algorithms' capability of reconstructing the neutron emissivity in general but also of detecting quick emissivity shape variations. The Tikhonov Regularization with first-order derivative and Minimum Fisher Information methods provide similar results within a minimal difference and detect correctly the change from peaked to flattened emissivity

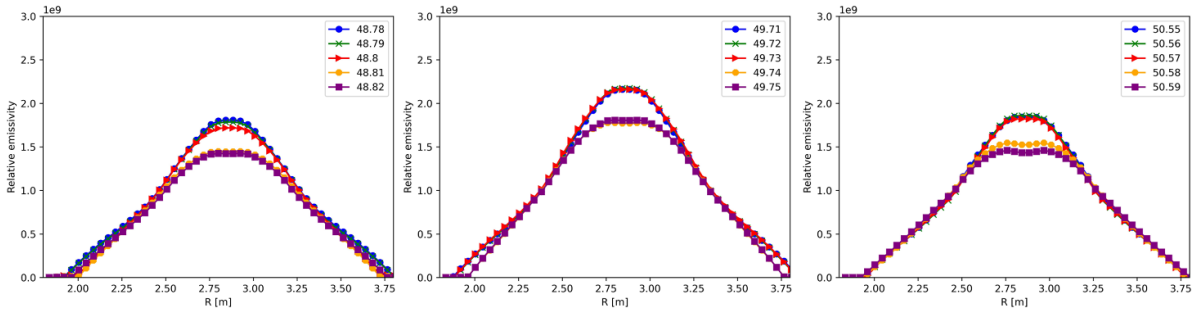


Figure 14. The time evolution of the neutron emissivity profiles around sawtooth crash in $t = 48.80$ s (left), 49.73 s (center), and 50.57 s (right) observed in discharge #99523 reconstructed by the TR method with the first-order derivative.

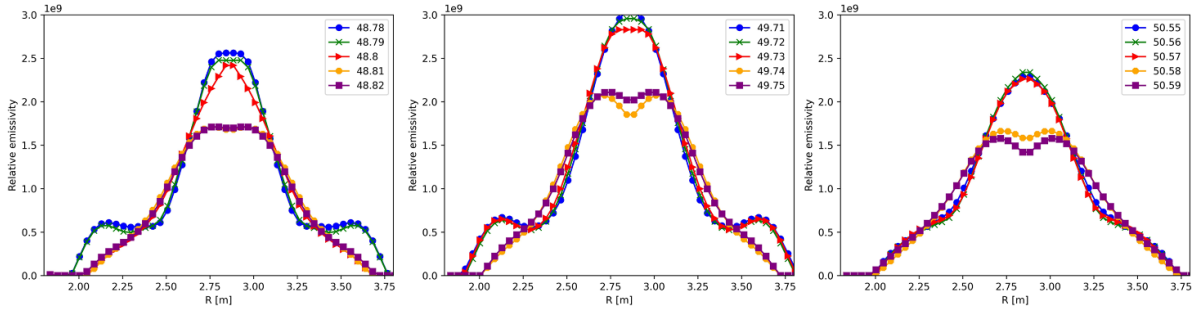


Figure 15. The time evolution of the neutron emissivity profiles around sawtooth crash in $t = 48.80$ s (left), 49.73 s (center), and 50.57 s (right) observed in discharge #99523 reconstructed by the TR method with the second-order derivative.

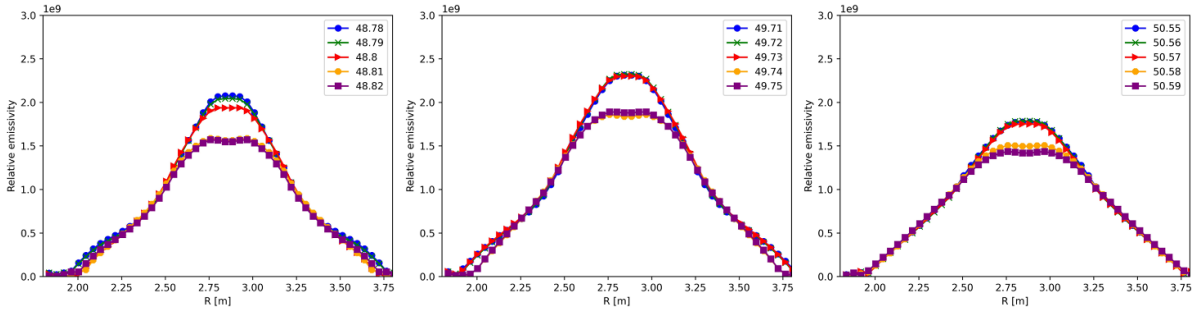


Figure 16. The time evolution of the neutron emissivity profiles around sawtooth crash in $t = 48.80$ s (left), 49.73 s (center), and 50.57 s (right) observed in discharge #99523 reconstructed by the MFI method.

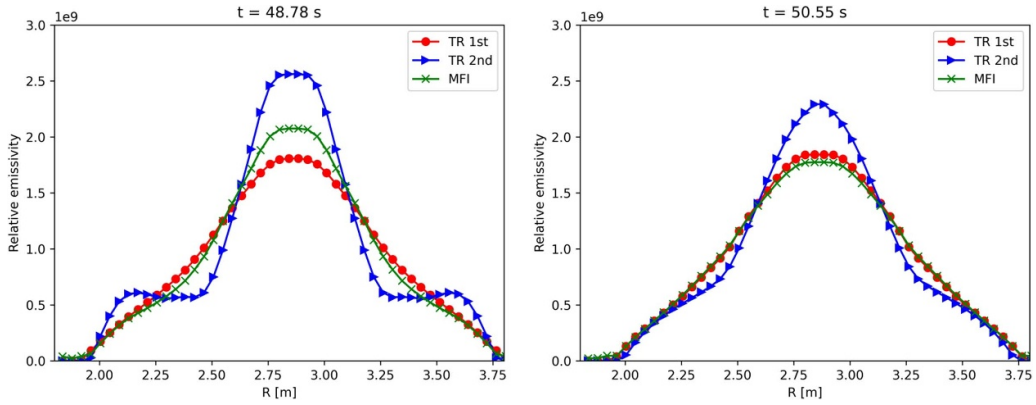


Figure 17. Comparison reconstruction capability of the three methods: peaked JET neutron emissivity profiles before sawtooth crashes at times $t = 48.78$ s (left) and $t = 50.55$ s (right).

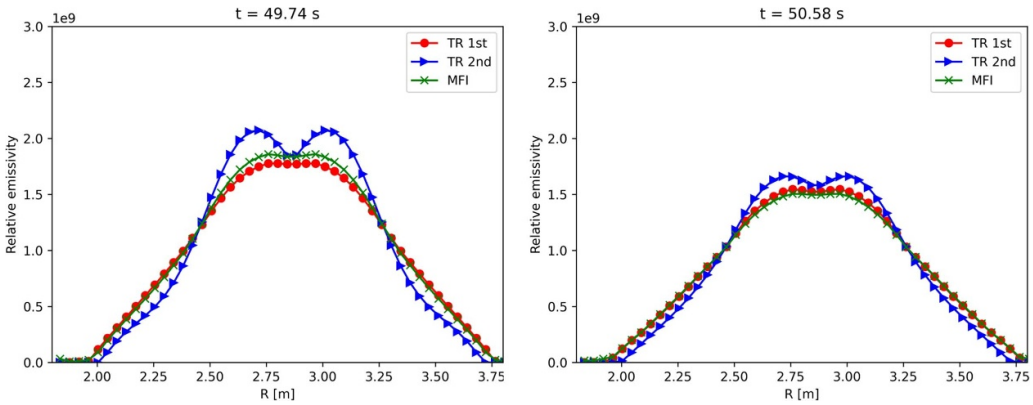


Figure 18. Comparison of the reconstruction capability of the three methods: flattened JET neutron emissivity profiles after sawtooth crashes at times $t = 49.74$ s (left) and $t = 50.58$ s (right).

and are therefore recommended for real-time implementation in the ITER RNC as well as for application in future experiments.

Data availability statement

The data cannot be made publicly available upon publication due to legal restrictions preventing unrestricted public distribution. The data that support the findings of this study are available upon reasonable request from the authors.

Acknowledgment

The work leading to this publication has been funded partially by Fusion for Energy under the Contract F4E-FPA-327. This publication reflects the views only of the author and Fusion for Energy cannot be held responsible for any use which may be made of the information contained therein.

This scientific paper has been published as part of the international project called 'PMW'. co-financed by the Polish Ministry of Science and Higher Education within the framework of the scientific financial resources for 2020-2024 under the Contract No 5111/ITER/2020/0.

This work has been carried out within the framework of the EUROfusion Consortium, funded by the European Union via the Euratom Research and Training Programme (Grant Agreement No 101052200—EUROfusion). Views and opinions expressed are however those of the author(s) only and do not necessarily reflect those of the European Union or the European Commission. Neither the European Union nor the European Commission can be held responsible for them. (Please mind the addendum 2019-2020).

Conflict of interest

The authors have no conflicts to disclose.

Author contributions

Katarzyna Mikszuta-Michalik: formal analysis, methodology, software, visualization, writing/review & editing (lead). Daniele Marocco: validation, supervision, writing/review & editing (supporting). Basilio Esposito: conceptualization, project administration, writing/review & editing (supporting).

ORCID iDs

Katarzyna Mikszuta-Michalik https://orcid.org/0000-0003-0845-6275
Basilio Esposito https://orcid.org/0000-0002-0005-5680

References

[1] Marocco D, Esposito B and Moro F 2020 Neutron measurements in ITER using the radial neutron camera *JINST* **7** C03033
[2] Esposito B *et al* 2022 Progress of Design and Development for the ITER Radial Neutron Camera *JOFE* **41** 22
[3] Mikszuta-Michalik K, Imrisek M, Esposito B, Marocco D, Mlynar J and Ficker O 2020 A total neutron yield constraint implemented to the RNC emissivity reconstruction on ITER tokamak *Fusion Eng. Des* **160** 111840
[4] Marocco D and Esposito B 2016 System level design and performances of the ITER radial neutron camera *Proc. 26th IAEA Fusion Energy Conf. Kyoto. FIP/P4-16* pp 4–16
[5] Cruz N *et al* 2019 The design and performance of the real-time software architecture for the ITER radial neutron camera *IEEE Trans. Nucl. Sci.* **66** 1310–7
[6] Mikszuta-Michalik K, Miklaszewski R, Gierlik M, Kwiatkowski R, Rzadkiewicz J and Szydłowski A 2021 Application of the different deconvolution methods to the neutron spectrum reconstruction from activation measurement *Fusion Eng. Des* **173** 112934
[7] Murari A *et al* 2005 New developments in JET neutron, γ-ray and particle diagnostics with relevance to ITER *Nucl. Fusion* **45** S195
[8] Mailloux J *et al* 2022 Overview of JET results for optimising ITER operation *Nucl. Fusion* **62** 042026

[9] Garzotti L *et al* 2019 Scenario development for D–T operation at JET *Nucl. Fusion* **59** 076037
[10] Aster R C, Borchers B and Thurber C H 2018 *Parameter Estimation and Inverse Problems* (Elsevier)
[11] Hansen P C 1992 Analysis of discrete ill-posed problems by means of the L-curve *SIAM Rev.* **34** 561–80
[12] Odstrcil M, Mlynar J, Odstrcil T, Alper B, Murari A and Contributors J E 2012 Modern numerical methods for plasma tomography optimization *Nucl. Instrum. Methods Phys. Res.* A **686** 156–61
[13] von der Linden W 1995 Maximum-entropy data analysis *Appl. Phys.* A **60** 155–65
[14] Shepp L A and Vardi Y 1982 Maximum likelihood reconstruction for emission tomography *IEEE Trans. Med. Imaging* **1** 113–22
[15] Marocco D, Esposito B and Moro F 2011 Combined unfolding and spatial inversion of neutron camera measurements for ion temperature profile determination in ITER *Nucl. Fusion* **51** 053011
[16] Polunovskiy E 2008 private communication
[17] Marcus F B *et al* 1991 JET neutron emission profiles and fast ion redistribution during sawtooth crashes *Plasma Phys. Control. Fusion* **33** 277
[18] Syme D B *et al* 2014 Fusion yield measurements on JET and their calibration *Fusion Eng. Des.* **89** 2766–75